Numerical Heat Transfer, Part A, 41: 529–546, 2002

1040-7782/02 $12.00 + .00

HYDROMAGNETIC COMBINED CONVECTION FLOW IN A VERTICAL LID-DRIVEN CAVITY WITH INTERNAL HEAT GENERATION OR ABSORPTION

Ali J. Chamkha
Department of Mechanical Engineering, Kuwait University, Safat, Kuwait

The problem of unsteady, laminar, combined forced-free convection flow in a square cavity in the presence of internal heat generation or absorption and a magnetic field is formulated. Both the top and bottom horizontal walls of the cavity are insulated while the left and right vertical walls are kept at constant and different temperatures. The left vertical wall is moving in its own plane at a constant speed while all other walls are fixed. A uniform magnetic field is applied in the horizontal direction normal to the moving wall. A temperature-dependent heat source or sink is assumed to exist within the cavity. The governing equations and conditions are solved numerically by the finite-volume approach along with the alternating direct implicit (ADI) procedure. Two cases of thermal boundary conditions corresponding to aiding and opposing flows are considered. Comparisons with previously published work are performed and the results are found to be in excellent agreement. A parametric study is conducted and a set of representative graphical results is presented and discussed to illustrate the influence of the physical parameters on the solution.

INTRODUCTION

Combined convection flow and heat transfer in cavities has possible applications in many engineering, technological, and natural processes. This includes nuclear reactors, solar ponds [1], lakes and reservoirs [2], solar collectors [3], and crystal growth [4]. Moreover, the flow and heat transfer in a shear- and buoyancy-driven cavity arises in industrial processes such as food processing and float glass production [5].

Combined forced-free convective flow in lid-driven cavities or enclosures occurs as a result of two competing mechanisms. The first is due to shear flow caused by the movement of one of the walls of the cavity while the second is due to buoyancy flow produced by thermal nonhomogeneity of the cavity boundaries. Understanding of these mechanisms is of great significance from technical and engineering standpoints. This problem has been used extensively as a benchmark case for the evaluation of numerical solution procedures for the Navier–Stokes equations [6–11]. Koseff and Street [12] studied experimentally as

Received 13 April 2001; accepted 2 October 2001.
Address correspondence to Ali J. Chamkha, Department of Mechanical Engineering, Kuwait University, P. O. Box 5969, Safat, 13060, Kuwait.

NOMENCLATURE

B_o	magnetic induction, Tesla
c_p	fluid specific heat, J/(kg. K)
g	gravitational acceleration, m/s^2
Gr	Grashof number, $g\beta\Delta TH^3/\nu^2$
H	cavity height, m
Ha^2	square of the Hartmann number, $\sigma B_o^2 H^2/\mu$
k	fluid thermal conductivity, W/(m. K.)
$\overline{\mathrm{Nu}}$	average Nusselt number at the moving wall, $\overline{\mathrm{Nu}} = -\int_0^1 \partial\theta/\partial X \mathrm{d}Y$
P	fluid pressure, Pa.
Pr	Prandtl number, ν/α
Q_o	heat generation or absorption coefficient
Re	Reynolds number, $U_o H/\nu$
T	temperature, °C
ΔT	temperature difference, $T_H - T_C$
t	time, s
u	velocity in the x-direction, m/s
U	dimensionless x-component of velocity, u/U_o
U_c	dimensionless velocity in the x-direction at midwidth of cavity
U_o	lid velocity, m/s
v	velocity in the y-direction, m/s
V	dimensionless y-component of velocity, v/U_o
V_c	dimensionless velocity in the y-direction at midheight of cavity
W	cavity width, m
x, y	Cartesian coordinates, m
X, Y	dimensionless Cartesian coordinates, $(x, y)/H$
α	fluid thermal diffusivity, m^2/s
β	coefficient of thermal expansion of fluid, K^{-1}
Δ	dimensionless heat generation or absorption coefficient, $Q_o H^2/\rho\alpha c_p$
μ	fluid dynamic viscosity, Pa. s
ν	fluid kinematic viscosity, μ/ρ_o
σ	fluid electrical conductivity
θ	dimensionless temperature, $(T - T_C)/(T_H - T_C)$
ψ	stream function, m^2/s
Ψ	dimensionless stream function, ψ/HU_o
Ω	dimensional vorticity, $\partial v/\partial x - \partial u/\partial y$
ω	dimensionless vorticity, $\Omega H/U_o$
τ	dimensionless time, tU_o/H
ρ_o	fluid density at reference temperature T_C

Subscripts

C	cold wall
H	hot wall

well as numerically the recirculation flow patterns for a wide range of Reynolds (Re) and Grashof (Gr) numbers. Their results showed that the three-dimensional features, such as corner eddies near the end walls, and Taylor–Gortler-like longitudinal vortices, have significant effects on the flow patterns for low Res. Both thermally stable and unstable lid-driven flows inside enclosures were investigated numerically by Torrance et al. [13] for fixed values of Res and Prs. Their numerical results indicated that the Richardson number, which represents the ratio of buoyancy to shear forces, is a controlling parameter for the problem. Prasad and Koseff [14] conducted an experimental investigation of recirculating flow caused by combined forced and natural convection heat transfer in a deep lid-driven cavity filled with water. For the range of the governing parameters studied, their results indicate that the overall heat transfer rate is a very weak function of the Gr for the examined range of the Re. The effects of the Prandtl number (Pr) on laminar mixed convection heat transfer in a lid-driven cavity were studied numerically by Moallemi and Jang [4]. Their numerical simulations revealed that the influence of the thermal buoyancy force on the flow and heat transfer inside cavities is predicted to be more pronounced for higher values of the fluid's Pr. Later on, Iwatsu et al. [15] analyzed numerically mixed convection heat transfer in a driven cavity with a stable vertical temperature gradient. Their results showed that the flow features are similar to those of a conventional driven cavity of a nonstratified fluid for small values of the Richardson number.

Also, it was found that for high values of the Richardson number, much of the fluid in both the middle and bottom portions of the cavity interior is stagnant. Khanafer and Chamkha [16] examined numerically mixed convection flow in a lid-driven enclosure filled with a fluid-saturated porous medium and reported on the effects of the Darcy and Richardson numbers on the flow and heat transfer characteristics. Recently, Aydin [17] investigated aiding and opposing mechanisms of mixed convection in a shear- and buoyancy-driven cavity and determined the range of the Richardson number for the forced-mixed-free convection regimes.

In recent years, there has been considerable interest in studying the influence of magnetic fields on the fluid flow dynamics and performance of various systems or processes employing electrically conducting fluids. For example, magetic fields have been used in crystal growth processes. Oreper and Szekely [18] found that the presence of a magnetic field can suppress natural convection currents and that the strength of the magnetic field is one of the important factors in determining the quality of the crystal. Ozoe and Maruo [19] investigated magnetic and gravitational natural convection of melted silicon two-dimensional numerical computations for the rate of heat transfer. Garandet et al. [20] and Alchaar et al. [21] studied natural convection heat transfer in a rectangular enclosure with a transverse magnetic field. The effect of a magnetic field on free convection in a rectangular enclosure has been studied by Rudraiah et al. [22] and Al-Najem et al. [23].

Convection heat transfer induced by internal heat generation has recently received considerable attention because of numerous applications in geophysics and energy-related engineering problems. Such applications include heat removal from nuclear fuel debris, underground disposal of radioactive waste materials, heat recovery from geothermal systems, particularly large storage systems of agricultural products and foodstuff, exothermic chemical reactions in packed-bed reactors, electric current in a semiconducting fluid such as glass and electrolyte, heating of flowing water in a solar collector, and radiative cooling of molten glass in a forehearth (see, for instance, Kakac et al. [24] and Song [25]). Acharya and Goldstein [26] studied numerically two-dimensional natural convection of air in an externally heated vertical or inclined square box containing uniformly distributed internal energy sources. Their numerical results showed two distinct flow pattern systems depending on the ratio of the internal to the external Rayleigh numbers. Also, it was found that the average heat flux ratio along the cold wall increased with increasing external Rayleigh numbers and decreasing internal Rayleigh numbers. Churbanov et al. [27] studied numerically unsteady natural convection of a heat generating fluid in a vertical rectangular enclosure with isothermal or adiabatic rigid walls. Khanafer and Chamkha [28] considered hydromagnetic natural convection from an inclined porous square enclosure with heat generation. They reported numerical results for various physical conditions. These results were obtained using a control volume-based finite-difference method in the two-dimensional stream function-vorticity formulation. More recently, Das and Sahoo [29] reported a pressure-velocity solution for natural convection for a fluid-saturated heat-generating porous medium in a square enclosure based on the finite-element method. It was observed that the peak temperature occurred at the

top central part and weaker velocity prevailed near the vertical walls of the enclosure due to the heat generation effect alone.

Motivated by previous works dealing with electrically conducting fluids in the presence of a magnetic field and/or a heat source or sink, the objective of the present work is to examine the influence of the Hartmann number, the heat generation or absorption coefficient, the Reynolds number, and the Grashof number on the characteristics of combined forced-free convection flow inside a square cavity having one of its vertical walls moving with a uniform speed. This will be done for two different thermal boundary conditions corresponding to both aiding and opposing flow situations.

PROBLEM FORMULATION

Consider unsteady, laminar, combined convection flow in a two-dimensional square cavity of height H and width W ($W = H$) filled with an electrically conducting fluid that generates or absorbs heat at a rate determined by the temperature difference between the fluid and the cold wall. The physical model and coordinate system considered in this investigation are shown in Figure 1. Both the top and bottom walls of the cavity are insulated while the left and the right walls

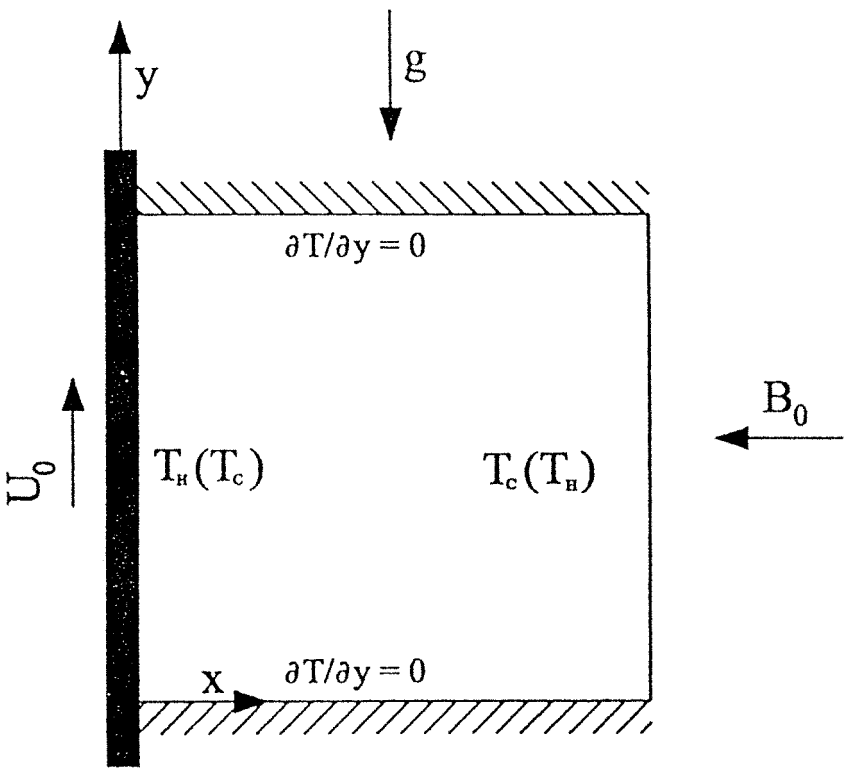

Figure 1. Schematic diagram of the physical system.

are maintained at constant and different temperatures, T_H and T_C, such that $T_H > T_C$. The left wall of the cavity is allowed to move in its own plane at a constant speed U_o. Two cases of thermal boundary conditions for the left and right walls are considered. The first is when the moving wall is the cold wall at T_C while the nonmoving wall is the hot wall at T_H (opposing flow). The second case is the opposite of the first where the moving wall is maintained at the hot temperature T_H while the nonmoving vertical wall is kept at the cold temperature T_C (aiding flow). While the fluid is assumed to be electrically conducting, all walls of the cavity are assumed to be electrically insulating. A uniform magentic field is applied in the horizontal direction normal to the moving wall. The magnetic Re is assumed to be small so that the induced magnetic field is neglected. The small magnetic Re assumption uncouples the Navier–Stokes equations from Maxwell's equations (see Cramer and Pai [30]). No electric field is present and the Hall effect is neglected. All fluid physical properties are assumed to be constant except the density variation in the body force term of the momentum equation according to the Boussinesq approximation. In addition, pressure work, viscous dissipation, and Joule heating are all assumed to be negligible.

The governing equations of the problem under consideration are based on the balance laws of mass, linear momentum, and energy modified to account for the presence of thermal buoyancy, magnetic field, and the heat generation or absorption effects. Taking into consideration the above-mentioned assumptions, we can write the dimensional form of these equations as

$$\frac{\partial u}{\partial x} + \frac{\partial v}{\partial y} = 0 \tag{1}$$

$$\frac{\partial u}{\partial t} + u\frac{\partial u}{\partial x} + v\frac{\partial u}{\partial y} = -\frac{1}{\rho_o}\frac{\partial P}{\partial x} + \nu\left(\frac{\partial^2 u}{\partial x^2} + \frac{\partial^2 u}{\partial y^2}\right) \tag{2}$$

$$\frac{\partial v}{\partial t} + u\frac{\partial v}{\partial x} + v\frac{\partial v}{\partial y} = -\frac{1}{\rho_o}\frac{\partial P}{\partial y} + \nu\left(\frac{\partial^2 v}{\partial x^2} + \frac{\partial^2 v}{\partial y^2}\right) + g\beta(T - T_C) - \frac{\sigma B_o^2 v}{\rho_o} \tag{3}$$

$$\frac{\partial T}{\partial t} + u\frac{\partial T}{\partial x} + v\frac{\partial T}{\partial y} = \frac{k}{\rho_o c_p}\left(\frac{\partial^2 T}{\partial x^2} + \frac{\partial^2 T}{\partial y^2}\right) + \frac{Q_o}{\rho_o c_p}(T - T_C) \tag{4}$$

where t is the time, and x and y are the coordinate directions. The variables u, v, P, and T are the fluid velocity components in the x- and y-directions, pressure, and temperature, respectively. The parameters β, σ, k, ν, ρ_o, and c_p are the fluid volumetric thermal expansion coefficient, electrical conductivity, thermal conductivity, kinematic viscosity, fluid density, and the specific heat, respectively. The parameters g, B_o and Q_o are the acceleration due to gravity, magnetic induction, and the volumetric internal heat generation ($Q_o > 0$) or absorption ($Q_o < 0$) coefficient, respectively.

The initial and boundary conditions for this problem can be written as follows:

$$\left.\begin{array}{l} u = v = 0 \quad T = 0 \quad \text{at all } x, y \text{ and } t < 0 \\ u = v = 0 \quad \text{on } x = 0, W \quad y = 0, H \\ \dfrac{\partial T}{\partial x} = 0 \quad \text{on } y = 0, H \\ \left.\begin{array}{l} T = T_C \quad \text{on } x = 0 \\ T = T_H \quad \text{on } x = W \end{array}\right\} \text{Case 1} \quad \text{for } t \geq 0 \\ \left.\begin{array}{l} T = T_H \quad \text{on } x = 0 \\ T = T_C \quad \text{on } x = W \end{array}\right\} \text{Case 2} \quad \text{for } t \geq 0 \end{array}\right\} \tag{5}$$

It is convenient to nondimensionalize Eqs. (1) through (5) using the following dimensionless variables:

$$\left.\begin{array}{ll} X = \dfrac{x}{H} & \mathrm{Y} = \dfrac{\mathrm{y}}{H} \\ \mathrm{U} = \dfrac{u}{U_o} & \mathrm{V} = \dfrac{v}{U_o} \\ \theta = \dfrac{T - T_C}{T_H - T_C} & \tau = \dfrac{tU_o}{H} \\ \omega = \dfrac{\Omega H}{U_o} & \Psi = \dfrac{\psi}{HU_o} \end{array}\right\} \tag{6}$$

where ψ and Ω are the dimensional stream function and vorticity, respectively.

Defining the stream function ψ and the vorticity Ω (see the nomenclature section) in the usual way and substituting Eqs. (6) into the previous governing equations results in the following dimensionless equations:

$$\omega = -\left(\frac{\partial^2 \Psi}{\partial X^2} + \frac{\partial^2 \Psi}{\partial Y^2}\right) \tag{7}$$

$$U = \frac{\partial \Psi}{\partial Y} \qquad V = -\frac{\partial \Psi}{\partial X} \tag{8}$$

$$\frac{\partial \omega}{\partial \tau} + U\frac{\partial \omega}{\partial X} + V\frac{\partial \omega}{\partial Y} = \frac{1}{\mathrm{Re}}\left(\frac{\partial^2 \omega}{\partial X^2} + \frac{\partial^2 \omega}{\partial Y^2}\right) + \frac{\mathrm{Gr}}{\mathrm{Re}^2}\frac{\partial \theta}{\partial X} - \frac{\mathrm{Ha}^2}{\mathrm{Re}}\frac{\partial V}{\partial X} \tag{9}$$

$$\frac{\partial \theta}{\partial \tau} + U\frac{\partial \theta}{\partial X} + V\frac{\partial \theta}{\partial Y} = \frac{1}{\mathrm{Pr\,Re}}\left(\frac{\partial^2 \theta}{\partial X^2} + \frac{\partial^2 \theta}{\partial Y^2}\right) + \frac{\Delta}{\mathrm{PrRe}}\theta \tag{10}$$

where $\mathrm{Re} = U_o H/\nu$, $\mathrm{Gr} = g\beta\Delta T H^3/\nu^2$, $\mathrm{Ha}^2 = \sigma B_o^2 H^2/\mu$, $\mathrm{Pr} = \nu/\alpha$, and $\Delta = Q_o H^2/\rho\alpha c_p$ (where $\Delta T = T_H - T_C$ and $\alpha = k/\rho C_p$ are the temperature difference and the thermal diffusivity, respectively) are the Re, Gr, square of the Hartmann number (Ha), Pr, and the dimensionless heat generation or absorption coefficient, respectively.

The dimensionless initial and boundary conditions of the problem under consideration can be written as

$$\begin{aligned} &U = V = \Psi = \theta = 0 && \text{for } \tau = 0 \\ &U = V = \Psi = 0 && \text{on all boundaries} \\ &\left.\begin{aligned} &\theta = 0 \quad \text{on } X = 0 \\ &\theta = 1 \quad \text{on } X = 1 \end{aligned}\right\} && \text{Case 1} \quad \text{for } \tau > 0 \\ &\left.\begin{aligned} &\theta = 1 \quad \text{on } X = 0 \\ &\theta = 0 \quad \text{on } X = 1 \end{aligned}\right\} && \text{Case 2} \quad \text{for } \tau > 0 \end{aligned} \tag{11}$$

Equations (9) and (10) governing ω and θ can be cast in the general canonical form (see Patankar [31]) as

$$\frac{\partial \phi}{\partial \tau} + \frac{\partial}{\partial X}\left[U\phi - \Gamma_\phi \frac{\partial \phi}{\partial X}\right] + \frac{\partial}{\partial Y}\left[V\phi - \Gamma_\phi \frac{\partial \phi}{\partial Y}\right] = S_\phi \tag{12}$$

where ϕ stands for ω or θ and Γ_ϕ and S_ϕ are given by

$$\begin{aligned} \Gamma_\theta &= \frac{1}{\mathrm{PrRe}} \qquad S_\theta = \frac{\Delta}{\mathrm{PrRe}} \\ \Gamma_\omega &= \frac{1}{\mathrm{Re}} \qquad S_\omega = \frac{\mathrm{Gr}}{\mathrm{Re}^2}\frac{\partial \theta}{\partial X} \frac{\mathrm{Ha}^2}{\mathrm{Re}}\frac{\partial V}{\partial X} \end{aligned} \tag{13}$$

The average Nusselt number at the moving wall of the cavity based on the conduction contribution may be expressed as

$$\overline{\mathrm{Nu}} = -\int_0^1 \frac{\partial \theta}{\partial X} \mathrm{d}Y \tag{14}$$

NUMERICAL ALGORITHM AND VALIDATION TESTS

In the present work, the boundary-value problem represented by Eqs. (7) through (10) is solved subject to its corresponding initial and boundary conditions given in Eqs. (11) by the control volume method discussed by Patankar [31]. In this method, the ADI procedure along with the successive grid refinement scheme are implemented in the spatial and temporal environments, respectively, to accelerate the convergence of the solution toward steady state. Additionally, the application of the ADI procedure enhances the accuracy of the solution since it allows the power-law scheme to be applied locally in a one-dimensional sense for each sweep in the coordinate directions.

In order to test and assess grid independence of the solution scheme, many numerical experiments were performed. These experiments showed that an equally spaced grid mesh of 81×81 is adequate to describe the flow and heat transfer characteristics accurately. Further increase in the number of grid points produced essentially the same results. The convergence criterion employed to reach the steady-

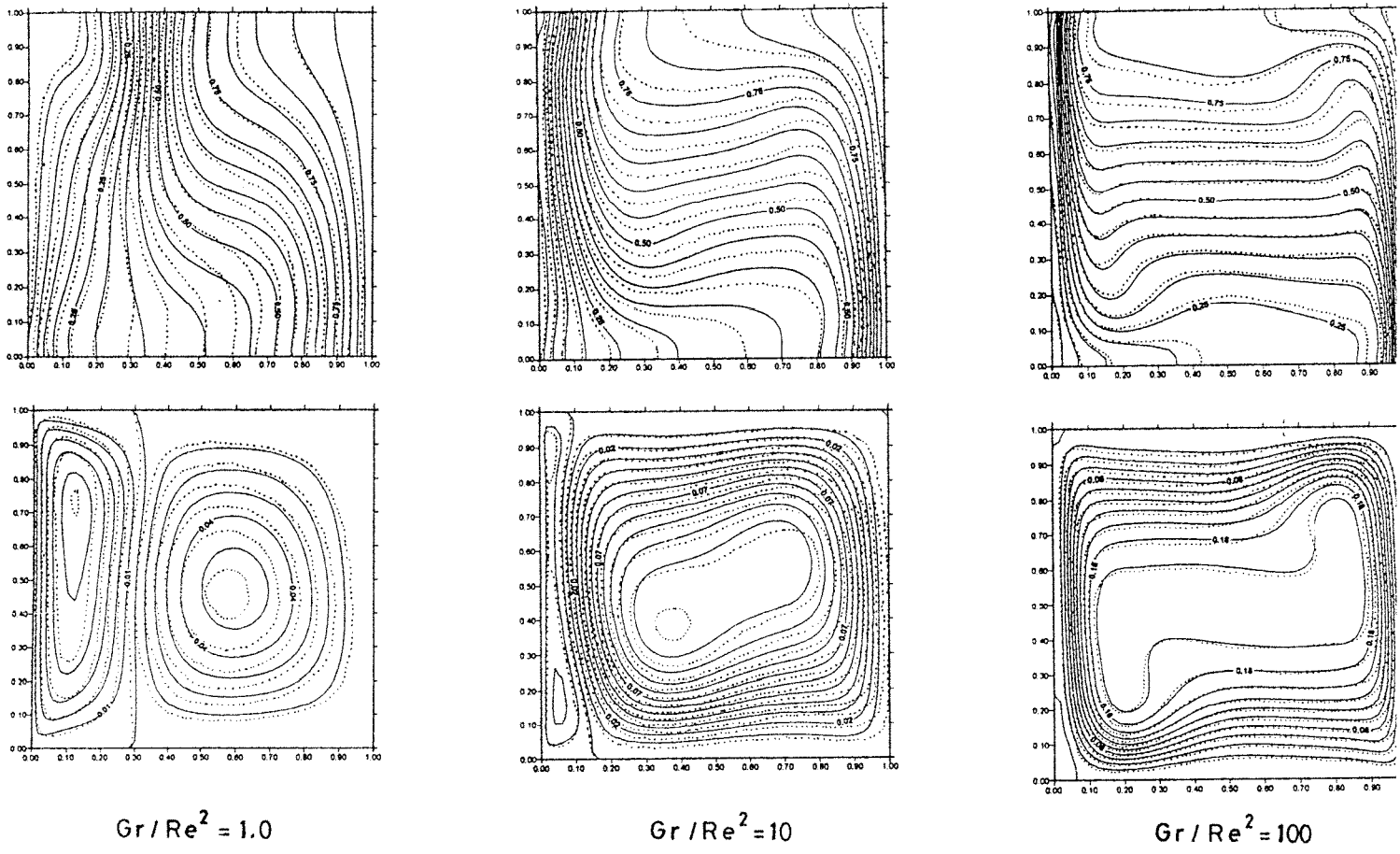

Figure 2. Comparison of present work with Aydin [17] for aiding flow (Case 2).

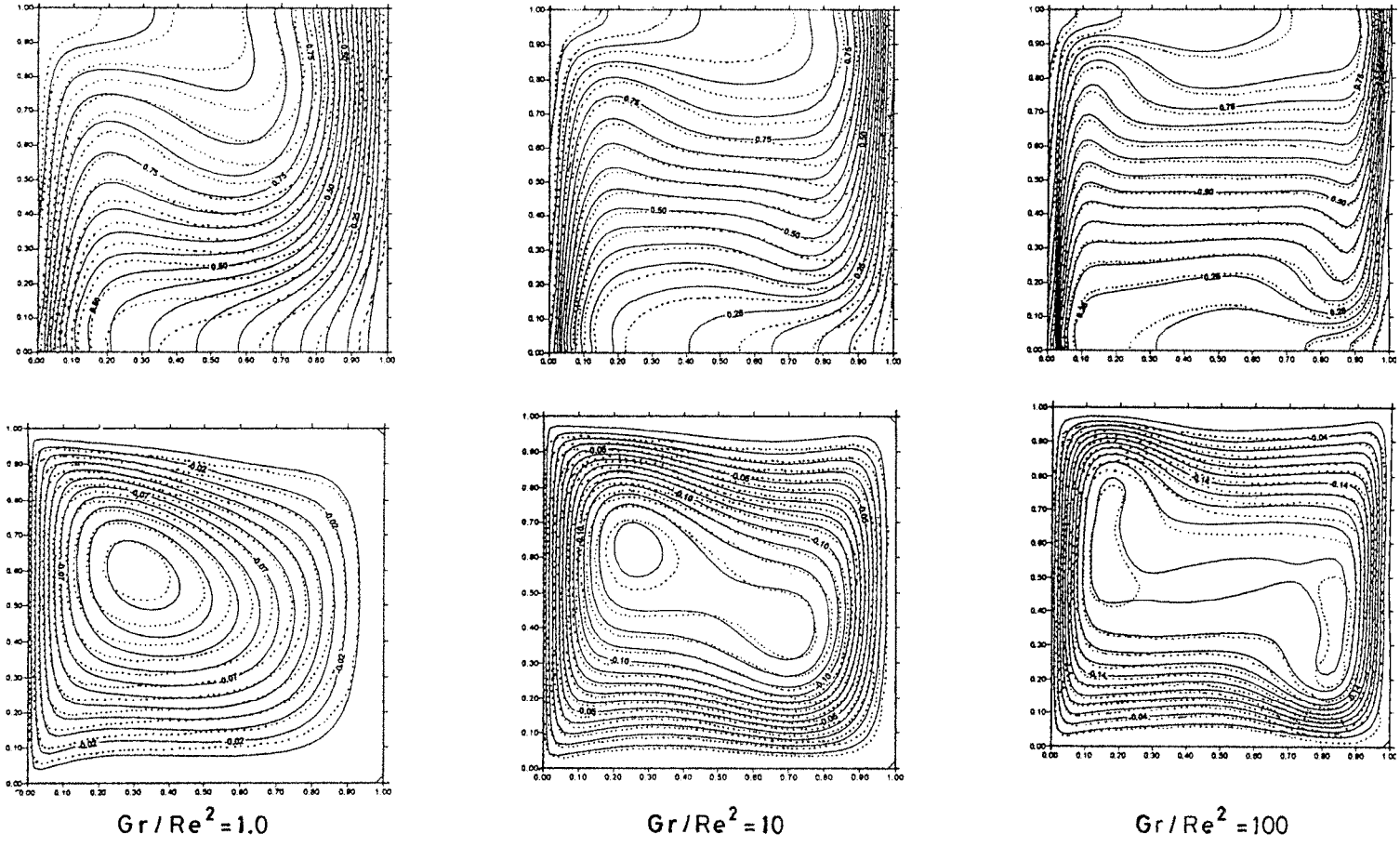

Figure 3. Comparison of present work with Aydin [17] for opposing flow (Case 1).

state solution was the standard relative error, which is based on the maximum norm given by

$$\delta = \frac{\|\Omega^{n+1} - \Omega^{n}\|_{\infty}}{\|\Omega^{n+1}\|_{\infty}} + \frac{\|\theta^{n+1} - \theta^{n}\|_{\infty}}{\|\theta^{n+1}\|_{\infty}} \leq 10^{-6} \tag{15}$$

where the operator $|\eta|_{\infty}$ indicates the maximum absolute value of the variable over all the grid points in the computational domain.

In order to verify the accuracy of the numerical results obtained throughout the present study, comparisons with the work of Aydin [17] were carried out by performing simulations for an Re Re = 100 and Gr Gr = 10^4, 10^5, and 10^6 in the absence of the magnetic (Ha = 0) and heat generation or absorption ($\Delta = 0$) effects. These comparisons for the contour maps of temperature and streamlines are presented in Figures 2 and 3 for aiding and opposing flow situations, respectively. In these figures, the solid lines correspond to the results of the present work while the dotted lines correspond to those of Aydin [17]. It is clear that excellent agreement between the present numerical solutions and those of Aydin [17] exists. As an additional check on the accuracy of the results, the convergence of the numerical solution is verified by performing an overall heat transfer balance inside the cavity. All of these favorable comparisons lend confidence to the accuracy of the numerical results of this work.

RESULTS AND DISCUSSION

In this section, the numerical results for combined convection heat transfer of a heat-generating or absorbing fluid in a vertical lid-driven square cavity in the presence of a transverse magnetic field are presented and discussed. By fixing the Pr at the value of 0.71, the controlling parameters for this investigation are the ratio Gr/Re^2 (sometimes called the Richardson number), Ha, and the dimensionless heat generation or absorption coefficient Δ.

Figure 4 displays typical temperature and streamlines contour maps for various values of Ha for an aiding flow situation (Case 2). In the absence of the magnetic field and the internal heat generation or absorption effects, the value of the Richardson number Gr/Re^2 provides a measure of the importance of buoyancy-driven natural convection relative to the lid-driven forced convection. For very small values of Gr/Re^2, Figure 4 indicates that the shear effect due to the movement of the left wall is dominant and that the flow features are similar to those of a viscous flow of a nonstratified fluid in a vertically driven cavity. The fluid flow is characterized by a primary recirculating eddy of the size of the cavity generated by the movement of the left wall and minor eddies near the right top and bottom corners. The temperature contour maps are clustered near the right vertical wall of the cavity resulting in steep temperature gradients there. In the remaining area of the cavity, the temperature gradients are small, which implies that the temperature differences are very small in the interior region of the cavity due to the vigorous effects of the shear-driven circulations. Application of a transverse magnetic field has the tendency to slow down the movement of the fluid in the cavity. This causes the flow circulation to progressively inhibit except in the region

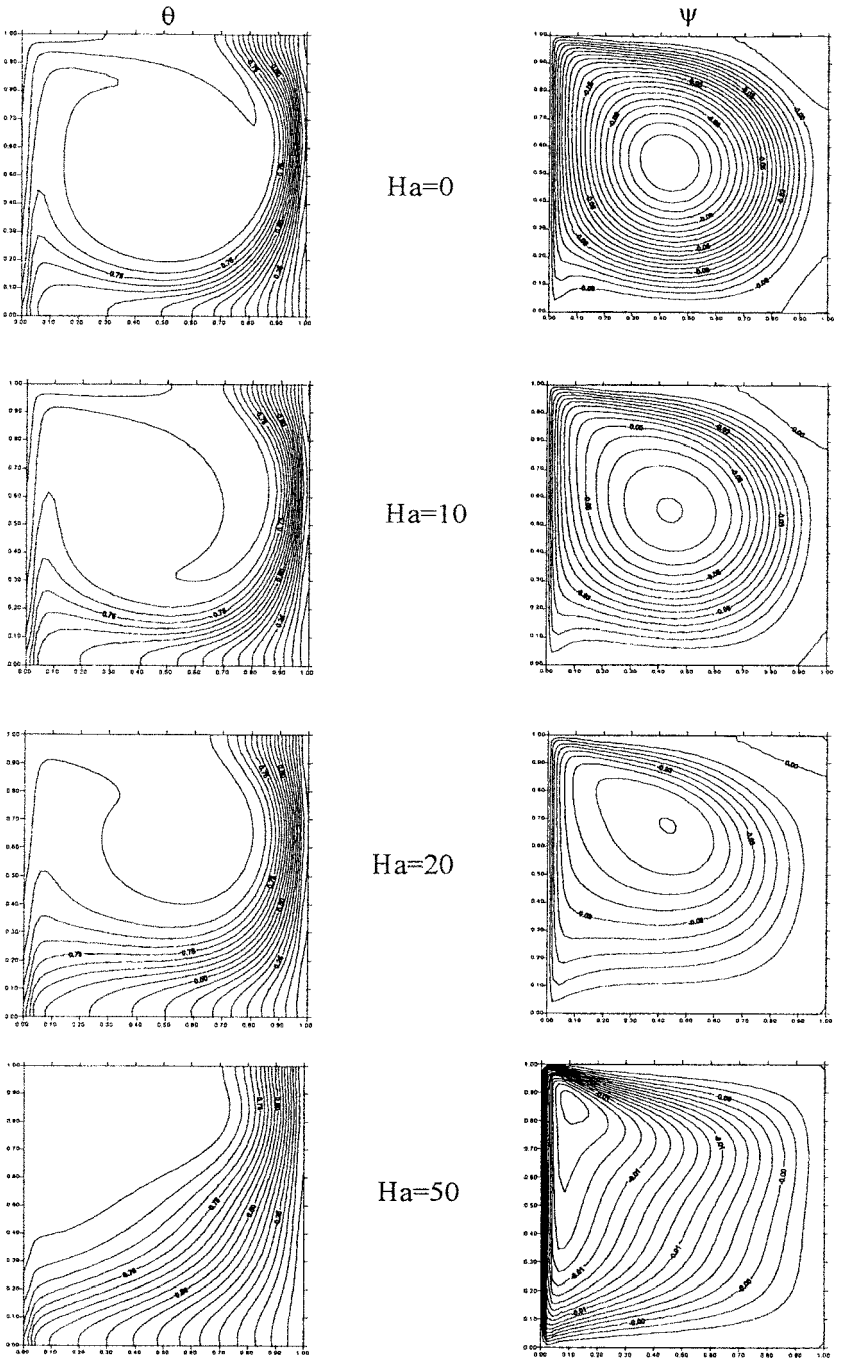

Figure 4. Effects of Ha on the streamlines and isotherms for aiding flow (Case 2), Gr = 100, Pr = 0.71, Re = 1000, and $\Delta = 0$.

close to the moving wall of the cavity. The minor eddies mentioned before disappear due to the presence of the magnetic field. The primary recirculating eddy tends to move closer and closer to the moving wall as the strength of the magnetic field increases further and further. In addition, the effect of the magnetic field is predicted to suppress the convective heat transfer mechanism and the isotherms become more parallel to the moving wall indicating the approach to a quasi-conduction regime. Moreover, the horizontal temperature stratification is substantially linear in the stagnant core of the cavity. This illustrates that the overall heat is transferred by conduction in the middle and close to the right wall of the cavity except in a relatively small region close to the moving wall where the induced convective activities are appreciable.

The effects of the internal heat generation or absorption coefficient Δ on the contour maps of temperature and streamlines for $Gr = 100$ and $Re = 1000$ are shown in Figure 5 for aiding flow (Case 2). In the absence of the internal heat generation or absorption effect, the maximum temperature occurs at the hot vertical wall. However, as the internal heat generation effect ($\Delta > 0$) increases, the boundary layer becomes more established along the vertical walls of the cavity, indicating sharp reductions in the temperature in the vicinity of these walls, and the maximum temperature tends to drift toward the center of the cavity. The temperature contour maps for $\Delta > 0$ illustrate the formation of a localized region of high temperature (relative to the hot wall temperature) in the core region between the hot and cold walls of the cavity. This is due to the fact that the hot fluid reaching the top insulated wall is unable to reject energy. In addition, it can be seen from this figure that the streamlines remain almost unchanged since they are controlled by the value of the Richardson number Gr/Re^2, which is very small in this figure. The presence of heat absorption ($\Delta < 0$) produces the opposite effect, where the high tempertaure region occurs close to the hot wall causing higher heat transfer rates.

The effect of the Ha on the velocity and the temperature profiles at the midsection of the vertical cavity for an aiding flow situation (Case 2) is depicted in Figures 6 through 8, respectively. Application of a transverse magnetic field in the horizontal direction normal to the vertical walls of the cavity results in a resistive force, which acts in the opposite vertical direction of the flow. This causes the horizontal velocity component in the upper region of the cavity to decrease and the vertical velocity component and temperature to increase. This is clearly noticed from the horizontal and vertical velocity profiles at the center of the cavity as depicted in Figures 6 through 8.

Finally, the effects of the Ha, the heat generation or absorption coefficient Δ, the Re, and the Gr on the average Nusselt number of the cavity $\overline{Nu}$ for both aiding (Case 2) and opposing (Case 1) flow situations are tabulated in Tables 1 through 4, respectively. It is observed that increases in the strength of the magnetic field cause decreases in the average Nusselt number for both aiding and opposing flow conditions. In addition, heat generation is predicted to decrease the average Nusselt number while heat absorption increases it for aiding flow. However, the opposite behavior is predicted for opposing flow. Moreover, for a fixed value of the Gr, increases in the value of the Re have the tendency to increase the convection heat transfer causing increases in the average Nusselt number. Furthermore, for a fixed value of the Re, increases in the value of the

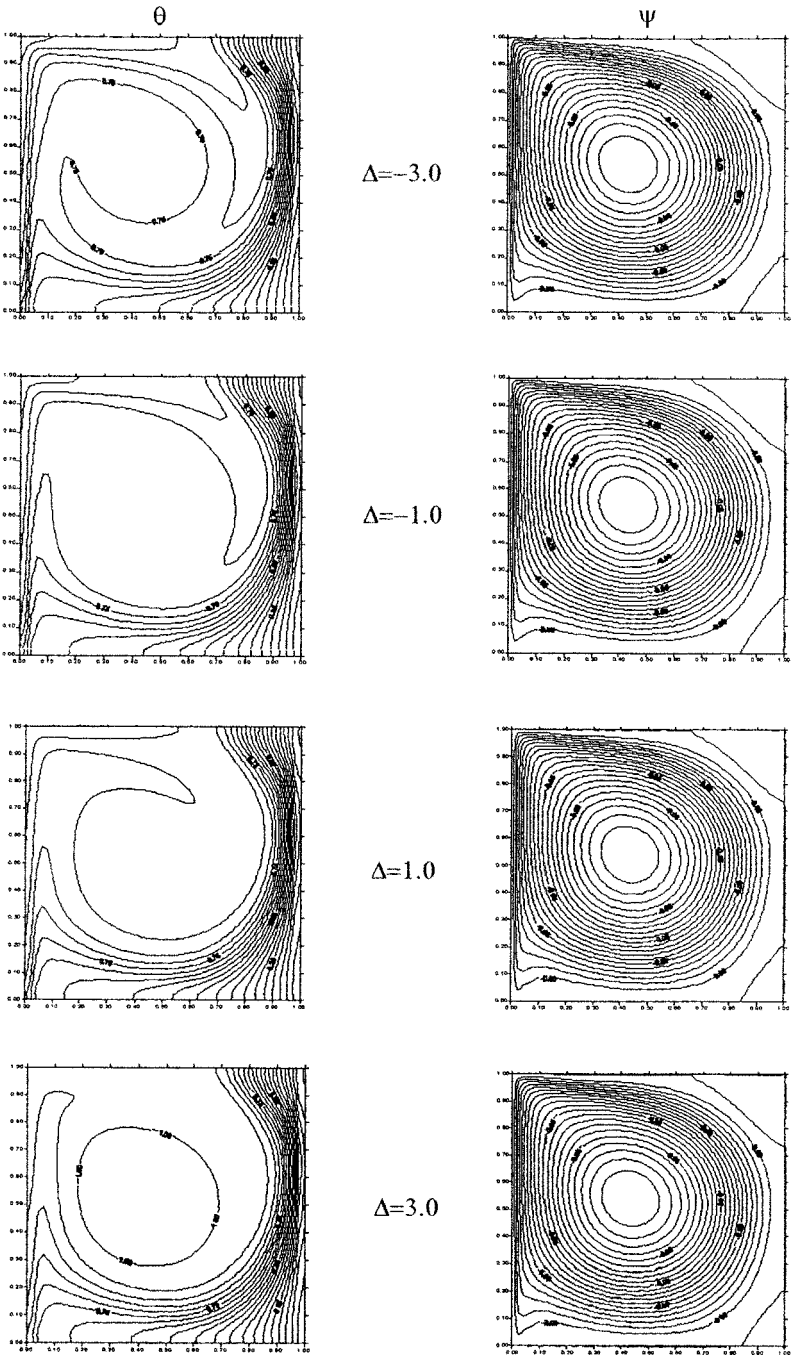

Figure 5. Effects of Δ on the streamlines and isotherms for aiding flow (Case 2), Gr = 100, Ha = 0, Pr = 0.71, and Re = 1000.

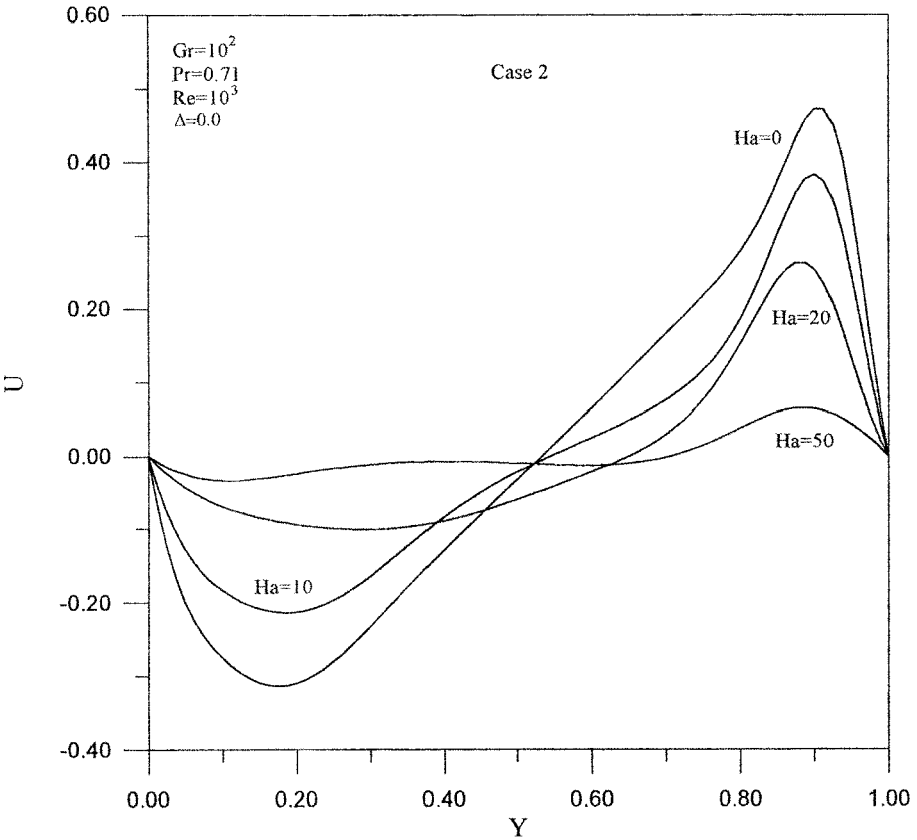

Figure 6. Effects of Ha on horizontal velocity profiles at enclosure midsection.

Gr (that is, increases in the value of the Richardson number Gr/Re^2) result in augmentation of the average Nusselt number for aiding flow. However, for opposing flow, the average Nusselt number is predicted to decrease as Gr is increased from 10^2 to 10^4 and to increase as Gr is increased beyond $Gr = 10^4$.

It is worth noting that under steady-state conditions and in the absence of heat generation or absorption effects, viscous dissipation, and Joule heating, an overall energy balance for the cavity considered shows that the average Nusselt number at the moving wall for aiding flow situations (Case 2) is the same as that for opposing flow situations (Case 1) but with the opposite sign. This is because in Case 1 heat transfers from the moving hot wall to the colder fluid while in Case 2 it transfers from the hot fluid (due to heating right wall) to the moving cold wall. This fact is demonstrated by Tables 1 and 2 for $\Delta = 0$. The slight difference in the numbers is probably due to the Nusselt number calculations at the corners of the cavity.

CONCLUSIONS

The problem of unsteady laminar combined convection flow and heat transfer of an electrically conducting and heat generating or absorbing fluid in a

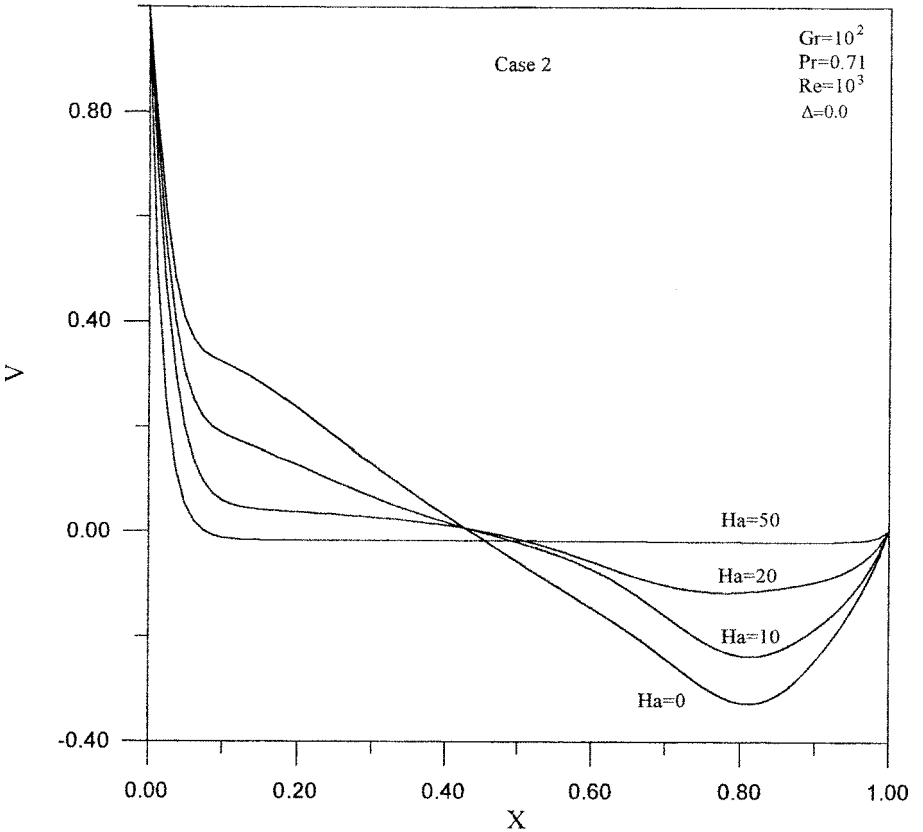

Figure 7. Effects of Ha on vertical velocity profiles at enclosure midsection.

vertical lid-driven cavity in the presence of a magnetic field was formulated. A numerical solution based on the finite-volume approach along with the ADI scheme was obtained. Comparisons with previously published work on special cases of the problem were performed and found to be in excellent agreement. A parametric study for both aiding and opposing flow conditions was conducted and the results were presented graphically and in tabulated form. It was found that the flow behavior and the heat transfer characteristics inside the cavity are strongly affected by the presence of the magnetic field. Significant reductions in the average Nusselt number were produced for both aiding and opposing flow situations as the strength of the applied magnetic field was increased. Moreover, the presence of the internal heat generation effects was found to decrease the average Nusselt number significantly for aiding flow and to increase it for opposing flow. The exact opposite behavior was predicted as a result of the presence of internal heat absorption effects. For a fixed value Gr, increasing the Re produced higher values in the average Nusselt number for both aiding and opposing flow conditions. On the other hand, for a fixed value of the Re, increases in the value of the Gr resulted in increasing the average Nusselt number for aiding flow.

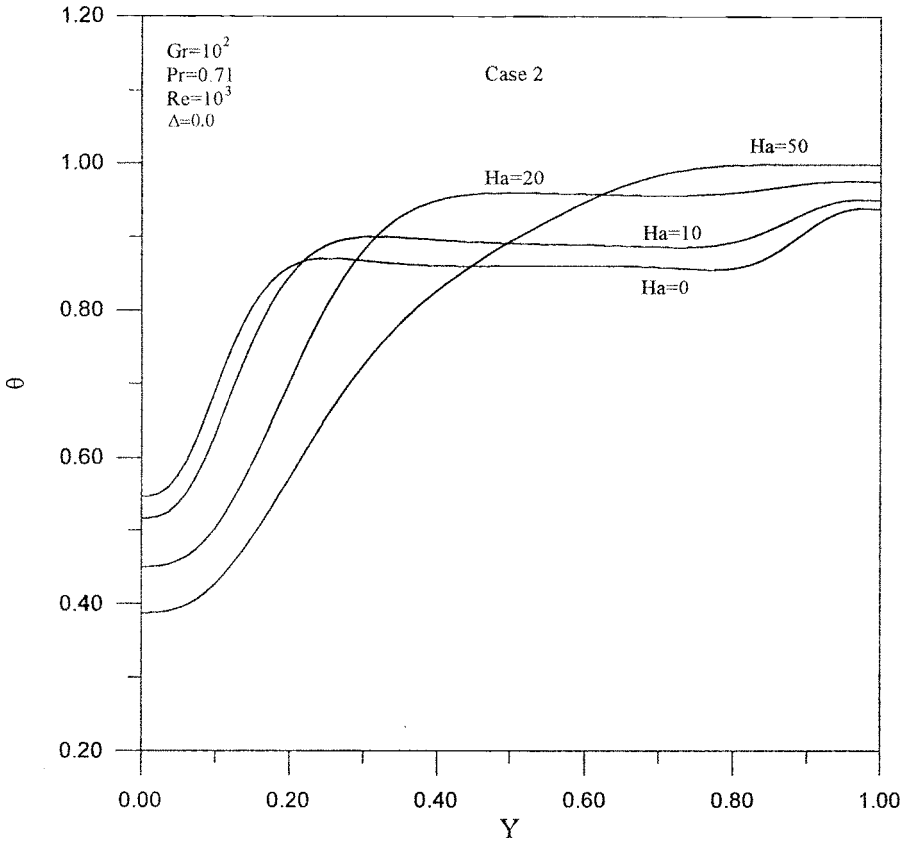

Figure 8. Effects of Ha on temperature profiles at enclosure midsection.

Table 1. Effects of Ha on the average Nusselt number at the left moving wall of the cavity for both aiding and opposing flow conditions for Gr = 100, Pr = 0.71, Re = 1000, and $\Delta = 0$

Parameter	$\overline{Nu}$ Opposing flow (Case 1)	$\overline{Nu}$ Aiding flow (Case 2)
Ha = 0.0	− 2.2678	2.2692
Ha = 10	− 2.1033	2.1050
Ha = 20	− 1.6452	1.6472
Ha = 50	− 0.9153	0.9164

Table 2. Effects of Δ on the average Nusselt number at the left moving wall of the cavity for both aiding and opposing flow conditions for Ha = 0, Gr = 100, Pr = 0.71, and Re = 1000

Parameter	$\overline{Nu}$ Opposing flow (Case 1)	$\overline{Nu}$ Aiding flow (Case 2)
$\Delta = -3.0$	− 2.1057	2.9052
$\Delta = -1.0$	− 2.2109	2.4963
$\Delta = 0.0$	− 2.2678	2.2692
$\Delta = 1.0$	− 2.3286	2.0245
$\Delta = 3.0$	− 2.4630	1.4727

Table 3. Effects of Re on the average Nusselt number at the left moving wall of the cavity for both aiding and opposing flow conditions for Ha = 0, Gr = 100, Pr = 0.71, and Δ = 0

Parameter	$\overline{Nu}$ opposing flow (Case 1)	$\overline{Nu}$ Aiding flow (Case 2)
Re = 100	− 0.9640	0.9819
Re = 400	− 1.6925	1.6971
Re = 1000	− 2.2678	2.2692

Table 4. Effects of Gr on the average Nusselt number at the left moving wall of the cavity for both aiding and opposing flow conditions for Ha = 0, Pr = 0.71, Re = 100, and Δ = 0

Parameter	$\overline{Nu}$ Opposing flow (Case 1)	$\overline{Nu}$ Aiding flow (Case 2)
$Gr = 10^2$	− 0.9640	0.9819
$Gr = 10^3$	− 0.8772	1.0554
$Gr = 10^4$	− 0.7398	1.4604
$Gr = 10^5$	− 1.6549	2.3620
$Gr = 10^6$	− 3.7434	4.0083

However, for opposing flow, as the Gr increased, the average Nusselt number initially decreased, reaching a minimum for $Gr = 10^4$ and then increased as the Gr was increased beyond this value.

REFERENCES

1. C. K. Cha and Y. Jaluria, Recirculating Mixed Convection Flow for Energy Extraction, *Int. J. Heat Mass Transfer*, vol. 27, pp. 1801–1810, 1984.
2. J. Imberger and P. F. Hamblin, Dynamics of Lakes, Reservoirs, and Cooling Ponds, *Annual Rev. Fluid Mech.*, vol. 14, pp. 153–187, 1982.
3. F. J. K. Ideriah, Prediction of Turbulent Cavity Flow Driven by Buoyancy and Shear, *J. Mech. Engng. Sci.*, vol. 22, pp. 287–295, 1980.
4. M. K. Moallemi and K. S. Jang, Prandtl Number Effects on Laminar Mixed Convection Heat Transfer in a Lid-Driven Cavity, *Int. J. Heat Mass Transfer*, vol. 35, pp. 1881–1892, 1992.
5. L. A. B. Pilkington, Review Lecture: The Float Glass Process, *Proc. Roy. Soc. Lond., A*, vol. 314, pp. 1–25, 1969.
6. R. K. Agarwal, A Third-Order-Accurate Upwind Scheme for Navier–Stokes Solutions at High Reynolds Numbers, AIAA-81-0112, *Proc. 19th AIAA Aerospace Sciences Meeting*, St. Louis, MO, January 1981.
7. D. L. Young, J. A. Liggett, and R. H. Gallagher, Unsteady Stratified Circulation in a Cavity, *ASCE J. The Engineering Mechanics Division*, vol. 102 (EM6), pp. 1009–1023, 1976.
8. M. Morzynski and Cz. O. Popiel, Laminar Heat Transfer in a Two-Dimensional Cavity Covered by a Moving Wall, *Numer. Heat Transfer*, vol. 13, pp. 265–273, 1988.
9. M. C. Thompson and J. H. Ferziger, An Adaptive Multigrid Technique for the Incompressible Navier–Stokes Equations, *J. Comput. Phys.*, vol. 82, pp. 94–121, 1989.
10. U. Ghia, K. N. Ghia, and C. T. Shin, High-Resolutions for Incompressible Flow Using Navier–Stokes Equations and a Multigrid Method, *J. Comput. Phys.*, vol. 48, pp. 387–411, 1982.
11. R. Schreiber and H. B. Keller, Driven Cavity Flows by Efficient Numerical Techniques, *J. Comput. Phys.*, vol. 49, pp. 310–333, 1983.
12. J. R. Kosef and R. L. Street, The Lid-Driven Cavity Flow: A Synthesis of Qualitative and Qualitative Observations, *ASME J. Fluids Engng.*, vol. 106, pp. 390–398, 1984.

13. K. Torrance, R. Davis, K. Elike, P. Gill, D. Gutman, A. Hsui, S. Lyons, and H. Zien, Cavity Flows Driven by Buoyancy and Shear, *J. Fluid Mech.*, vol. 51, pp. 221–231, 1972.
14. A. K. Prasad and J. R. Koseff, Combined Forced and Natural Convection Heat Transfer in a Deep Lid-Driven Cavity Flow, in *Heat Transfer in Convective Flows*, HTD-107, pp. 155–162, ASME, New York, 1989.
15. R. Iwatsu, J. M. Hyun, and K. Kuwahara, Mixed Convection in a Driven Cavity with a Stable Vertical Temperature Gradient, *Int. J. Heat Mass Transfer*, vol. 36, pp. 1601–1608, 1993.
16. K. Khanafer and A. J. Chamkha, Mixed Convection Flow in a Lid-Driven Enclosure Filled with a Fluid-Saturated Porous Medium, *Int. J. Heat Mass Transfer*, vol. 42, pp. 2465–2481, 1999.
17. O. Aydin, Aiding and Opposing Mechanisms of Mixed Convection in a Shear- and Buoyancy-Driven Cavity, *Int. Commun. Heat Mass Transfer*, vol. 26, pp. 1019–1028, 1999.
18. G. M. Oreper and J. Szekely, The Effect of an Externally Imposed Magnetic Field on Buoyancy Driven Flow in a Rectangular Cavity, *Journal of Crystal Growth*, vol. 64, pp. 505–515, 1983.
19. H. Ozoe and M. Maruo, Magnetic and Gravitational Natural Convection of Melted Silicon-Two Dimensional Numerical Computations for the Rate of Heat Transfer, *JSME*, vol. 30, pp. 774–784, 1987.
20. J. P. Garandet, T. Alboussiere, and R. Moreau, Buoyancy Driven Convection in a Rectangular Enclosure with a Transverse Magnetic Field, *Int. J. Heat Mass Transfer*, vol. 35, pp. 741–748, 1992.
21. S. Alchaar, P. Vasseur, and E. Bilgen, Natural Convection Heat Transfer in a Rectangular Enclosure with a Transverse Magnetic Field, *ASME Journal of Heat Transfer*, vol. 117, pp. 668–673, 1995.
22. N. Rudraiah, R. M. Barron, M. Venkatachalappa, and C. K. Subbaraya, Effect of a Magnetic Field on Free Convection in a Rectangular Enclosure, *Int. J. Engng Sci.*, vol. 33, pp. 1075–1084, 1995.
23. N. Al-Najem, K. Khanafer, and M. El-Refaee, Numerical Study of Laminar Natural Convection in Tilted Enclosure with Transverse Magnetic Field, *Int. J. Numerical Methods for Heat and Fluid Flow*, vol. 8, pp. 651–672, 1998.
24. S. Kakac, W. Aung, and R. Viskanta, *Natural Convection-Fundamentals and Applications*, Hemisphere, Washington, DC, 1985.
25. T.-H. Song, Stability of a Fluid Layer with Uniform Heat Generation and Convection Boundary Conditions, *Int. J. Heat Mass Transfer*, vol. 39, pp. 2378–2382, 1996.
26. S. Acharya and R. J. Goldstein, Natural Convection in an Externally Heated Vertical or Inclined Square Box Containing Internal Energy Sources, *ASME J. Heat Transfer*, vol. 107, pp. 855–866, 1985.
27. A. G. Churbanov, P. N. Vabishchevich, V. V. Chudanov, and V. F. Strizhov, A Numerical Study on Natural Convection of a Heat-Generating Fluid in Rectangular Enclosures, *Int. J. Heat Mass Transfer*, vol. 37, pp. 2969–2984, 1994.
28. K. Khanafer and A. J. Chamkha, Hydomagnetic Natural Convection from an Inclined Porous Square Enclosure with Heat Generation, *Numerical Heat Transfer*, vol. 33, pp. 891–910, 1998.
29. S. Das and R. K. Sahoo, Effect of Darcy, Fluid Rayleigh and Heat Generation Parameters on Natural Convection in a Porous Square Enclosure: A Brinkman-Extended Darcy Model, *Int. Commun. Heat Mass Transfer*, vol. 26, pp. 569–578, 1999.
30. K. R. Cramer and S.-I. Pai, *Magnetofluid Dynamics for Engineers and Applied Physicists*, Scripta Publishing Company, Washington, DC, 1973.
31. S. V. Patankar, *Numerical Heat Transfer and Fluid Flow*, Hemisphere, Washington, DC, 1980.